

Measurement of the branching fraction of the doubly Cabibbo-suppressed decay $D^0 \rightarrow K^+\pi^-\pi^0$ and search for $D^0 \rightarrow K^+\pi^-\pi^0\pi^0$

M. Ablikim¹, M. N. Achasov^{10,b}, P. Adlarson⁶⁸, M. Albrecht⁴, R. Aliberti²⁸, A. Amoroso^{67A,67C}, M. R. An³², Q. An^{64,50}, X. H. Bai⁵⁸, Y. Bai⁴⁹, O. Bakina²⁹, R. Baldini Ferroli^{23A}, I. Balossino^{24A}, Y. Ban^{39,g}, V. Batozskaya^{1,37}, D. Becker²⁸, K. Begzsuren²⁶, N. Berger²⁸, M. Bertani^{23A}, D. Bettoni^{24A}, F. Bianchi^{67A,67C}, J. Bloms⁶¹, A. Bortone^{67A,67C}, I. Boyko²⁹, R. A. Briere⁵, A. Brueggemann⁶¹, H. Cai⁶⁹, X. Cai^{1,50}, A. Calcaterra^{23A}, G. F. Cao^{1,55}, N. Cao^{1,55}, S. A. Cetin^{54A}, J. F. Chang^{1,50}, W. L. Chang^{1,55}, G. Chelkov^{29,a}, C. Chen³⁶, G. Chen¹, H. S. Chen^{1,55}, M. L. Chen^{1,50}, S. J. Chen³⁵, T. Chen¹, X. R. Chen^{25,55}, X. T. Chen¹, Y. B. Chen^{1,50}, Z. J. Chen^{20,h}, W. S. Cheng^{67C}, G. Cibinetto^{24A}, F. Cossio^{67C}, J. J. Cui⁴², H. L. Dai^{1,50}, J. P. Dai⁷¹, A. Dbeyssi¹⁴, R. E. de Boer⁴, D. Dedovich²⁹, Z. Y. Deng¹, A. Denig²⁸, I. Denysenko²⁹, M. Destefanis^{67A,67C}, F. De Mori^{67A,67C}, Y. Ding³³, J. Dong^{1,50}, L. Y. Dong^{1,55}, M. Y. Dong^{1,50,55}, X. Dong⁶⁹, S. X. Du⁷³, P. Egorov^{29,a}, Y. L. Fan⁶⁹, J. Fang^{1,50}, S. S. Fang^{1,55}, Y. Fang¹, R. Farinelli^{24A}, L. Fava^{67B,67C}, F. Feldbauer⁴, G. Felici^{23A}, C. Q. Feng^{64,50}, J. H. Feng⁵¹, K. Fischer⁶², M. Fritsch⁴, C. D. Fu¹, H. Gao⁵⁵, Y. N. Gao^{39,g}, Yang Gao^{64,50}, S. Garbolino^{67C}, I. Garzia^{24A,24B}, P. T. Ge⁶⁹, Z. W. Ge³⁵, C. Geng⁵¹, E. M. Gersabeck⁵⁹, A. Gilman⁶², K. Goetzen¹¹, L. Gong³³, W. X. Gong^{1,50}, W. Gradl²⁸, M. Greco^{67A,67C}, L. M. Gu³⁵, M. H. Gu^{1,50}, C. Y. Guan^{1,55}, A. Q. Guo^{25,55}, L. B. Guo³⁴, R. P. Guo⁴¹, Y. P. Guo^{9,f}, A. Guskov^{29,a}, T. T. Han⁴², W. Y. Han³², X. Q. Hao¹⁵, F. A. Harris⁵⁷, K. K. He⁴⁷, K. L. He^{1,55}, F. H. Heinsius⁴, C. H. Heinz²⁸, Y. K. Heng^{1,50,55}, C. Herold⁵², M. Himmelreich^{11,d}, T. Holtmann⁴, G. Y. Hou^{1,55}, Y. R. Hou⁵⁵, Z. L. Hou¹, H. M. Hu^{1,55}, J. F. Hu^{48,i}, T. Hu^{1,50,55}, Y. Hu¹, G. S. Huang^{64,50}, K. X. Huang⁵¹, L. Q. Huang⁶⁵, L. Q. Huang^{25,55}, X. T. Huang⁴², Y. P. Huang¹, Z. Huang^{39,g}, T. Hussain⁶⁶, N. Hüsken^{22,28}, W. Imoehl²², M. Irshad^{64,50}, J. Jackson²², S. Jaeger⁴, S. Janchiv²⁶, Q. Ji¹, Q. P. Ji¹⁵, X. B. Ji^{1,55}, X. L. Ji^{1,50}, Y. Y. Ji⁴², Z. K. Jia^{64,50}, H. B. Jiang⁴², S. S. Jiang³², X. S. Jiang^{1,50,55}, Y. Jiang⁵⁵, J. B. Jiao⁴², Z. Jiao¹⁸, S. Jin³⁵, Y. Jin⁵⁸, M. Q. Jing^{1,55}, T. Johansson⁶⁸, N. Kalantar-Nayestanaki⁵⁶, X. S. Kang³³, R. Kappert⁵⁶, M. Kavatsyuk⁵⁶, B. C. Ke⁷³, I. K. Keshk⁴, A. Khokkaz⁶¹, P. Kiese²⁸, R. Kiuchi¹, R. Kliemt¹¹, L. Koch³⁰, O. B. Kolcu^{54A}, B. Kopf⁴, M. Kuemmel⁴, M. Kuessner⁴, A. Kupsc^{37,68}, W. Kühn³⁰, J. J. Lane⁵⁹, J. S. Lange³⁰, P. Larin¹⁴, A. Lavanaia²¹, L. Lavezzi^{67A,67C}, Z. H. Lei^{64,50}, H. Leithoff²⁸, M. Lellmann²⁸, T. Lenz²⁸, C. Li⁴⁰, C. Li³⁶, C. H. Li³², Cheng Li^{64,50}, D. M. Li⁷³, F. Li^{1,50}, G. Li¹, H. Li⁴⁴, H. Li^{64,50}, H. B. Li^{1,55}, H. J. Li¹⁵, H. N. Li^{48,i}, J. Q. Li⁴, J. S. Li⁵¹, J. W. Li⁴², Ke Li¹, L. J Li¹, L. K. Li¹, Lei Li³, M. H. Li³⁶, P. R. Li^{31,j,k}, S. X. Li⁹, S. Y. Li⁵³, T. Li⁴², W. D. Li^{1,55}, W. G. Li¹, X. H. Li^{64,50}, X. L. Li⁴², Xiaoyu Li^{1,55}, H. Liang^{1,55}, H. Liang^{64,50}, H. Liang²⁷, Y. F. Liang⁴⁶, Y. T. Liang^{25,55}, G. R. Liao¹², L. Z. Liao⁴², J. Libby²¹, A. Limphirat⁵², C. X. Lin⁵¹, D. X. Lin^{25,55}, T. Lin¹, B. J. Liu¹, C. X. Liu¹, D. Liu^{14,64}, F. H. Liu⁴⁵, Fang Liu¹, Feng Liu⁶, G. M. Liu^{48,i}, H. M. Liu^{1,55}, Huanhuan Liu¹, Huihui Liu¹⁶, J. B. Liu^{64,50}, J. L. Liu⁶⁵, J. Y. Liu^{1,55}, K. Liu¹, K. Y. Liu³³, Ke Liu¹⁷, L. Liu^{64,50}, M. H. Liu^{9,f}, P. L. Liu¹, Q. Liu⁵⁵, S. B. Liu^{64,50}, T. Liu^{9,f}, W. K. Liu³⁶, W. M. Liu^{64,50}, X. Liu^{31,j,k}, Y. Liu^{31,j,k}, Y. B. Liu³⁶, Z. A. Liu^{1,50,55}, Z. Q. Liu⁴², X. C. Lou^{1,50,55}, F. X. Lu⁵¹, H. J. Lu¹⁸, J. G. Lu^{1,50}, X. L. Lu¹, Y. Lu¹, Y. P. Lu^{1,50}, Z. H. Lu¹, C. L. Luo³⁴, M. X. Luo⁷², T. Luo^{9,f}, X. L. Luo^{1,50}, X. R. Lyu⁵⁵, Y. F. Lyu³⁶, F. C. Ma³³, H. L. Ma¹, L. L. Ma⁴², M. M. Ma^{1,55}, Q. M. Ma¹, R. Q. Ma^{1,55}, R. T. Ma⁵⁵, X. Y. Ma^{1,50}, Y. Ma^{39,g}, F. E. Maas¹⁴, M. Maggiora^{67A,67C}, S. Maldaner⁴, S. Malde⁶², Q. A. Malik⁶⁶, A. Mangoni^{23B}, Y. J. Mao^{39,g}, Z. P. Mao¹, S. Marcello^{67A,67C}, Z. X. Meng⁵⁸, J. G. Messchendorp^{56,11}, G. Mezzadri^{24A}, H. Miao¹, T. J. Min³⁵, R. E. Mitchell²², X. H. Mo^{1,50,55}, N. Yu. Muchnoi^{10,b}, H. Muramatsu⁶⁰, S. Nakhoul^{11,d}, Y. Nefedov²⁹, F. Nerling^{11,d}, I. B. Nikolaev^{10,b}, Z. Ning^{1,50}, S. Nisar^{8,l}, Y. Niu⁴², S. L. Olsen⁵⁵, Q. Ouyang^{1,50,55}, S. Pacetti^{23B,23C}, X. Pan^{9,f}, Y. Pan⁵⁹, A. Pathak¹, A. Pathak²⁷, M. Pelizaeus⁴, H. P. Peng^{64,50}, K. Peters^{11,d}, J. Pettersson⁶⁸, J. L. Ping³⁴, R. G. Ping^{1,55}, S. Plura²⁸, S. Pogodin²⁹, R. Poling⁶⁰, V. Prasad^{64,50}, H. Qi^{64,50}, H. R. Qi⁵³, M. Qi³⁵, T. Y. Qi^{9,f}, S. Qian^{1,50}, W. B. Qian⁵⁵, Z. Qian⁵¹, C. F. Qiao⁵⁵, J. J. Qin⁶⁵, L. Q. Qin¹², X. P. Qin^{9,f}, X. S. Qin⁴², Z. H. Qin^{1,50}, J. F. Qiu¹, S. Q. Qu³⁶, S. Q. Qu⁵³, K. H. Rashid⁶⁶, K. Ravindran²¹, C. F. Redmer²⁸, K. J. Ren³², A. Rivetti^{67C}, V. Rodin⁵⁶, M. Rolo^{67C}, G. Rong^{1,55}, Ch. Rosner¹⁴, M. Rump⁶¹, H. S. Sang⁶⁴, A. Sarantsev^{29,c}, Y. Schelhaas²⁸, C. Schmier⁴, K. Schoenning⁶⁸, M. Scodreggio^{24A,24B}, K. Y. Shan^{9,f}, W. Shan¹⁹, X. Y. Shan^{64,50}, J. F. Shangguan⁴⁷, L. G. Shao^{1,55}, M. Shao^{64,50}, C. P. Shen^{9,f}, H. F. Shen^{1,55}, X. Y. Shen^{1,55}, B.-A. Shi⁵⁵, H. C. Shi^{64,50}, R. S. Shi^{1,55}, X. Shi^{1,50}, X. D Shi^{64,50}, J. J. Song¹⁵, W. M. Song^{27,1}, Y. X. Song^{39,g}, S. Sosio^{67A,67C}, S. Spataro^{67A,67C}, F. Stieler²⁸, K. X. Su⁶⁹, P. P. Su⁴⁷, Y.-J. Su⁵⁵, G. X. Sun¹, H. Sun⁵⁵, H. K. Sun¹, J. F. Sun¹⁵, L. Sun⁶⁹, S. S. Sun^{1,55}, T. Sun^{1,55}, W. Y. Sun²⁷, X Sun^{20,h}, Y. J. Sun^{64,50}, Y. Z. Sun¹, Z. T. Sun⁴², Y. H. Tan⁶⁹, Y. X. Tan^{64,50}, C. J. Tang⁴⁶, G. Y. Tang¹, J. Tang⁵¹, L. Y. Tao⁶⁵, Q. T. Tao^{20,h}, J. X. Teng^{64,50}, V. Thoren⁶⁸, W. H. Tian⁴⁴, Y. Tian^{25,55}, I. Uman^{54B}, B. Wang¹, B. L. Wang⁵⁵, C. W. Wang³⁵, D. Y. Wang^{39,g}, F. Wang⁶⁵, H. J. Wang^{31,j,k}, H. P. Wang^{1,55}, K. Wang^{1,50}, L. L. Wang¹,

M. Wang⁴², M. Z. Wang^{39,g}, Meng Wang^{1,55}, S. Wang^{9,f}, T. Wang^{9,f}, T. J. Wang³⁶, W. Wang⁵¹, W. H. Wang⁶⁹, W. P. Wang^{64,50}, X. Wang^{39,g}, X. F. Wang^{31,j,k}, X. L. Wang^{9,f}, Y. D. Wang³⁸, Y. F. Wang^{1,50,55}, Y. H. Wang⁴⁰, Y. Q. Wang¹, Z. Wang^{1,50}, Z. Y. Wang^{1,55}, Ziyi Wang⁵⁵, D. H. Wei¹², F. Weidner⁶¹, S. P. Wen¹, D. J. White⁵⁹, U. Wiedner⁴, G. Wilkinson⁶², M. Wolke⁶⁸, L. Wollenberg⁴, J. F. Wu^{1,55}, L. H. Wu¹, L. J. Wu^{1,55}, X. Wu^{9,f}, X. H. Wu²⁷, Y. Wu⁶⁴, Z. Wu^{1,50}, L. Xia^{64,50}, T. Xiang^{39,g}, G. Y. Xiao³⁵, H. Xiao^{9,f}, S. Y. Xiao¹, Y. L. Xiao^{9,f}, Z. J. Xiao³⁴, C. Xie³⁵, X. H. Xie^{39,g}, Y. Xie⁴², Y. G. Xie^{1,50}, Y. H. Xie⁶, Z. P. Xie^{64,50}, T. Y. Xing^{1,55}, C. F. Xu¹, C. J. Xu⁵¹, G. F. Xu¹, H. Y. Xu⁵⁸, Q. J. Xu¹³, S. Y. Xu⁶³, X. P. Xu⁴⁷, Y. C. Xu⁵⁵, Z. P. Xu³⁵, F. Yan^{9,f}, L. Yan^{9,f}, W. B. Yan^{64,50}, W. C. Yan⁷³, H. J. Yang^{43,e}, H. L. Yang²⁷, H. X. Yang¹, L. Yang⁴⁴, S. L. Yang⁵⁵, Y. X. Yang^{1,55}, Yifan Yang^{1,55}, M. Ye^{1,50}, M. H. Ye⁷, J. H. Yin¹, Z. Y. You⁵¹, B. X. Yu^{1,50,55}, C. X. Yu³⁶, G. Yu^{1,55}, J. S. Yu^{20,h}, T. Yu⁶⁵, C. Z. Yuan^{1,55}, L. Yuan², S. C. Yuan¹, X. Q. Yuan¹, Y. Yuan^{1,55}, Z. Y. Yuan⁵¹, C. X. Yue³², A. A. Zafar⁶⁶, F. R. Zeng⁴², X. Zeng Zeng⁶, Y. Zeng^{20,h}, Y. H. Zhan⁵¹, A. Q. Zhang¹, B. L. Zhang¹, B. X. Zhang¹, G. Y. Zhang¹⁵, H. Zhang⁶⁴, H. H. Zhang⁵¹, H. H. Zhang²⁷, H. Y. Zhang^{1,50}, J. L. Zhang⁷⁰, J. Q. Zhang³⁴, J. W. Zhang^{1,50,55}, J. Y. Zhang¹, J. Z. Zhang^{1,55}, Jianyu Zhang^{1,55}, Jiawei Zhang^{1,55}, L. M. Zhang⁵³, L. Q. Zhang⁵¹, Lei Zhang³⁵, P. Zhang¹, Q. Y. Zhang^{32,73}, Shulei Zhang^{20,h}, X. D. Zhang³⁸, X. M. Zhang¹, X. Y. Zhang⁴², X. Y. Zhang⁴⁷, Y. Zhang⁶², Y. T. Zhang⁷³, Y. H. Zhang^{1,50}, Yan Zhang^{64,50}, Yao Zhang¹, Z. H. Zhang¹, Z. Y. Zhang⁶⁹, Z. Y. Zhang³⁶, G. Zhao¹, J. Zhao³², J. Y. Zhao^{1,55}, J. Z. Zhao^{1,50}, Lei Zhao^{64,50}, Ling Zhao¹, M. G. Zhao³⁶, Q. Zhao¹, S. J. Zhao⁷³, Y. B. Zhao^{1,50}, Y. X. Zhao^{25,55}, Z. G. Zhao^{64,50}, A. Zhemchugov^{29,a}, B. Zheng⁶⁵, J. P. Zheng^{1,50}, Y. H. Zheng⁵⁵, B. Zhong³⁴, C. Zhong⁶⁵, X. Zhong⁵¹, H. Zhou⁴², L. P. Zhou^{1,55}, X. Zhou⁶⁹, X. K. Zhou⁵⁵, X. R. Zhou^{64,50}, X. Y. Zhou³², Y. Z. Zhou^{9,f}, J. Zhu³⁶, K. Zhu¹, K. J. Zhu^{1,50,55}, L. X. Zhu⁵⁵, S. H. Zhu⁶³, S. Q. Zhu³⁵, T. J. Zhu⁷⁰, W. J. Zhu^{9,f}, Y. C. Zhu^{64,50}, Z. A. Zhu^{1,55}, B. S. Zou¹, J. H. Zou¹

(BESIII Collaboration)

¹ *Institute of High Energy Physics, Beijing 100049, People's Republic of China*

² *Beihang University, Beijing 100191, People's Republic of China*

³ *Beijing Institute of Petrochemical Technology, Beijing 102617, People's Republic of China*

⁴ *Bochum Ruhr-University, D-44780 Bochum, Germany*

⁵ *Carnegie Mellon University, Pittsburgh, Pennsylvania 15213, USA*

⁶ *Central China Normal University, Wuhan 430079, People's Republic of China*

⁷ *China Center of Advanced Science and Technology, Beijing 100190, People's Republic of China*

⁸ *COMSATS University Islamabad, Lahore Campus, Defence Road, Off Raiwind Road, 54000 Lahore, Pakistan*

⁹ *Fudan University, Shanghai 200433, People's Republic of China*

¹⁰ *G.I. Budker Institute of Nuclear Physics SB RAS (BINP), Novosibirsk 630090, Russia*

¹¹ *GSI Helmholtzcentre for Heavy Ion Research GmbH, D-64291 Darmstadt, Germany*

¹² *Guangxi Normal University, Guilin 541004, People's Republic of China*

¹³ *Hangzhou Normal University, Hangzhou 310036, People's Republic of China*

¹⁴ *Helmholtz Institute Mainz, Staudinger Weg 18, D-55099 Mainz, Germany*

¹⁵ *Henan Normal University, Xinxiang 453007, People's Republic of China*

¹⁶ *Henan University of Science and Technology, Luoyang 471003, People's Republic of China*

¹⁷ *Henan University of Technology, Zhengzhou 450001, People's Republic of China*

¹⁸ *Huangshan College, Huangshan 245000, People's Republic of China*

¹⁹ *Hunan Normal University, Changsha 410081, People's Republic of China*

²⁰ *Hunan University, Changsha 410082, People's Republic of China*

²¹ *Indian Institute of Technology Madras, Chennai 600036, India*

²² *Indiana University, Bloomington, Indiana 47405, USA*

²³ *INFN Laboratori Nazionali di Frascati, (A)INFN Laboratori Nazionali di Frascati, I-00044, Frascati, Italy; (B)INFN Sezione di Perugia, I-06100, Perugia, Italy; (C)University of Perugia, I-06100, Perugia, Italy*

²⁴ *INFN Sezione di Ferrara, (A)INFN Sezione di Ferrara, I-44122, Ferrara, Italy; (B)University of Ferrara, I-44122, Ferrara, Italy*

²⁵ *Institute of Modern Physics, Lanzhou 730000, People's Republic of China*

²⁶ *Institute of Physics and Technology, Peace Ave. 54B, Ulaanbaatar 13330, Mongolia*

²⁷ *Jilin University, Changchun 130012, People's Republic of China*

²⁸ *Johannes Gutenberg University of Mainz, Johann-Joachim-Becher-Weg 45, D-55099 Mainz, Germany*

²⁹ *Joint Institute for Nuclear Research, 141980 Dubna, Moscow region, Russia*

³⁰ *Justus-Liebig-Universitaet Giessen, II. Physikalisches Institut, Heinrich-Buff-Ring 16, D-35392 Giessen, Germany*

- ³¹ Lanzhou University, Lanzhou 730000, People's Republic of China
- ³² Liaoning Normal University, Dalian 116029, People's Republic of China
- ³³ Liaoning University, Shenyang 110036, People's Republic of China
- ³⁴ Nanjing Normal University, Nanjing 210023, People's Republic of China
- ³⁵ Nanjing University, Nanjing 210093, People's Republic of China
- ³⁶ Nankai University, Tianjin 300071, People's Republic of China
- ³⁷ National Centre for Nuclear Research, Warsaw 02-093, Poland
- ³⁸ North China Electric Power University, Beijing 102206, People's Republic of China
- ³⁹ Peking University, Beijing 100871, People's Republic of China
- ⁴⁰ Qufu Normal University, Qufu 273165, People's Republic of China
- ⁴¹ Shandong Normal University, Jinan 250014, People's Republic of China
- ⁴² Shandong University, Jinan 250100, People's Republic of China
- ⁴³ Shanghai Jiao Tong University, Shanghai 200240, People's Republic of China
- ⁴⁴ Shanxi Normal University, Linfen 041004, People's Republic of China
- ⁴⁵ Shanxi University, Taiyuan 030006, People's Republic of China
- ⁴⁶ Sichuan University, Chengdu 610064, People's Republic of China
- ⁴⁷ Soochow University, Suzhou 215006, People's Republic of China
- ⁴⁸ South China Normal University, Guangzhou 510006, People's Republic of China
- ⁴⁹ Southeast University, Nanjing 211100, People's Republic of China
- ⁵⁰ State Key Laboratory of Particle Detection and Electronics, Beijing 100049, Hefei 230026, People's Republic of China
- ⁵¹ Sun Yat-Sen University, Guangzhou 510275, People's Republic of China
- ⁵² Suranaree University of Technology, University Avenue 111, Nakhon Ratchasima 30000, Thailand
- ⁵³ Tsinghua University, Beijing 100084, People's Republic of China
- ⁵⁴ Turkish Accelerator Center Particle Factory Group, (A)Istinye University, 34010, Istanbul, Turkey; (B)Near East University, Nicosia, North Cyprus, Mersin 10, Turkey
- ⁵⁵ University of Chinese Academy of Sciences, Beijing 100049, People's Republic of China
- ⁵⁶ University of Groningen, NL-9747 AA Groningen, The Netherlands
- ⁵⁷ University of Hawaii, Honolulu, Hawaii 96822, USA
- ⁵⁸ University of Jinan, Jinan 250022, People's Republic of China
- ⁵⁹ University of Manchester, Oxford Road, Manchester, M13 9PL, United Kingdom
- ⁶⁰ University of Minnesota, Minneapolis, Minnesota 55455, USA
- ⁶¹ University of Muenster, Wilhelm-Klemm-Str. 9, 48149 Muenster, Germany
- ⁶² University of Oxford, Keble Rd, Oxford, UK OX13RH
- ⁶³ University of Science and Technology Liaoning, Anshan 114051, People's Republic of China
- ⁶⁴ University of Science and Technology of China, Hefei 230026, People's Republic of China
- ⁶⁵ University of South China, Hengyang 421001, People's Republic of China
- ⁶⁶ University of the Punjab, Lahore-54590, Pakistan
- ⁶⁷ University of Turin and INFN, (A)University of Turin, I-10125, Turin, Italy; (B)University of Eastern Piedmont, I-15121, Alessandria, Italy; (C)INFN, I-10125, Turin, Italy
- ⁶⁸ Uppsala University, Box 516, SE-75120 Uppsala, Sweden
- ⁶⁹ Wuhan University, Wuhan 430072, People's Republic of China
- ⁷⁰ Xinyang Normal University, Xinyang 464000, People's Republic of China
- ⁷¹ Yunnan University, Kunming 650500, People's Republic of China
- ⁷² Zhejiang University, Hangzhou 310027, People's Republic of China
- ⁷³ Zhengzhou University, Zhengzhou 450001, People's Republic of China
- ^a Also at the Moscow Institute of Physics and Technology, Moscow 141700, Russia
- ^b Also at the Novosibirsk State University, Novosibirsk, 630090, Russia
- ^c Also at the NRC "Kurchatov Institute", PNPI, 188300, Gatchina, Russia
- ^d Also at Goethe University Frankfurt, 60323 Frankfurt am Main, Germany
- ^e Also at Key Laboratory for Particle Physics, Astrophysics and Cosmology, Ministry of Education; Shanghai Key Laboratory for Particle Physics and Cosmology; Institute of Nuclear and Particle Physics, Shanghai 200240, People's Republic of China

^f Also at Key Laboratory of Nuclear Physics and Ion-beam Application (MOE) and Institute of Modern Physics, Fudan University, Shanghai 200443, People's Republic of China

^g Also at State Key Laboratory of Nuclear Physics and Technology, Peking University, Beijing 100871, People's Republic of China

^h Also at School of Physics and Electronics, Hunan University, Changsha 410082, China

ⁱ Also at Guangdong Provincial Key Laboratory of Nuclear Science, Institute of Quantum Matter, South China Normal University, Guangzhou 510006, China

^j Also at Frontiers Science Center for Rare Isotopes, Lanzhou University, Lanzhou 730000, People's Republic of China

^k Also at Lanzhou Center for Theoretical Physics, Lanzhou University, Lanzhou 730000, People's Republic of China

^l Also at the Department of Mathematical Sciences, IBA, Karachi, Pakistan

Using 2.93 fb^{-1} of e^+e^- collision data collected at a center-of-mass energy of 3.773 GeV with the BESIII detector, we present a measurement of the branching fraction of the doubly Cabibbo-suppressed (DCS) decay $D^0 \rightarrow K^+\pi^-\pi^0$ and a search for the DCS decay $D^0 \rightarrow K^+\pi^-\pi^0\pi^0$. The branching fraction of $D^0 \rightarrow K^+\pi^-\pi^0$ is determined to be $[3.13_{-0.56}^{+0.60}(\text{stat}) \pm 0.09(\text{syst})] \times 10^{-4}$. No signal is observed for $D^0 \rightarrow K^+\pi^-\pi^0\pi^0$ and an upper limit of 3.6×10^{-4} is set on the branching fraction at the 90% C.L. We combine these results with the world-average branching fractions of their counterpart Cabibbo-favored decays to determine the ratios of the doubly Cabibbo-suppressed over the Cabibbo-favored branching fractions, $\mathcal{B}(D^0 \rightarrow K^+\pi^-\pi^0)/\mathcal{B}(D^0 \rightarrow K^-\pi^+\pi^0) = (0.22 \pm 0.04)\%$ and $\mathcal{B}(D^0 \rightarrow K^+\pi^-\pi^0\pi^0)/\mathcal{B}(D^0 \rightarrow K^-\pi^+\pi^0\pi^0) < 0.40\%$ at the 90% C.L., which correspond to $(0.75 \pm 0.14) \tan^4 \theta_C$ and $1.37 \times \tan^4 \theta_C$, respectively, where θ_C is the Cabibbo angle.

PACS numbers: 13.20.Fc, 14.40.Lb

I. INTRODUCTION

Studies of doubly Cabibbo-suppressed (DCS) decays of charmed mesons provide important information on charmed-hadron dynamics. The ratio of the branching fraction of a given DCS $D^{0(+)}$ decay relative to its Cabibbo-favored (CF) counterpart is naively expected to be about $(0.5 - 2) \times \tan^4 \theta_C$ (θ_C is the Cabibbo mixing angle) [1, 2]. Recently, BESIII reported the observation of the DCS decay $D^+ \rightarrow K^+\pi^+\pi^-\pi^0$ [3, 4] (charge conjugate processes are implied throughout this paper). The branching fraction of this decay averaged over the two measurements reported in Refs. [3, 4] is $[1.13 \pm 0.08(\text{stat}) \pm 0.03(\text{syst})] \times 10^{-3}$, which gives a DCS/CF branching fraction ratio of $(6.28 \pm 0.52) \tan^4 \theta_C$. Comprehensive measurements of the DCS decays of other charmed mesons, especially for isospin symmetrical decays of D^0 , may shed light on the origin of this anomalously large DCS/CF branching fraction ratio.

So far, only a few DCS D^0 decays, namely $D^0 \rightarrow K^+\pi^-$, $D^0 \rightarrow K^+\pi^-\pi^0$ and $D^0 \rightarrow K^+\pi^-\pi^-\pi^+$, have been observed, with decay branching fractions extracted from the ratio of DCS/CF decay branching fractions from the experiments determining D^0 - \bar{D}^0 mixing parameters or coherence parameters [5]. In this paper, we present the first direct measurements of the branching fractions of $D^0 \rightarrow K^+\pi^-\pi^0$ and $D^0 \rightarrow K^+\pi^-\pi^0\pi^0$ by analyzing 2.93 fb^{-1} of e^+e^- collision data [6] taken at a center-of-mass energy of 3.773 GeV with the BESIII detector. Because the traditional hadronic tag method suffers from complex quantum-correlation effects [7], this analysis is performed with the semileptonic tag method adopted in our previous work [4]. Our direct measurements would benefit the constraint of the charm mixing parameters

when combining with individual CF D^0 decay branching fraction.

II. DATA AND MONTE CARLO

The BESIII detector is a magnetic spectrometer [8] located at the Beijing Electron Positron Collider (BEPCII) [9]. The cylindrical core of the BESIII detector consists of a helium-based multilayer drift chamber (MDC), a plastic scintillator time-of-flight system (TOF), and a CsI(Tl) electromagnetic calorimeter (EMC), which are all enclosed in a superconducting solenoidal magnet providing a 1.0 T magnetic field. The solenoid is supported by an octagonal flux-return yoke with resistive plate counter muon-identifier modules interleaved with steel. The acceptance of charged particles and photons is 93% over the 4π solid angle. The charged-particle momentum resolution at 1 GeV/c is 0.5%, and the resolution of specific ionization energy loss (dE/dx) is 6% for electrons from Bhabha scattering. The EMC measures photon energies with a resolution of 2.5% (5%) at 1 GeV in the barrel (end-cap) region. The time resolution of the TOF barrel part is 68 ps, while that of the end-cap part is 110 ps. Details about the design and performance of the BESIII detector are given in Ref. [8].

Simulated samples produced with the GEANT4-based [10] Monte Carlo (MC) package, which includes the geometric description of the BESIII detector and the detector response, are used to determine the detection efficiency and to estimate the backgrounds. The simulation includes the beam-energy spread and initial-state radiation in the e^+e^- annihilations modeled

with the generator KKMC [11]. The inclusive MC samples consist of the production of $D\bar{D}$ pairs, the non- $D\bar{D}$ decays of the $\psi(3770)$, the initial-state radiation production of the J/ψ and $\psi(3686)$ states, and the continuum processes. The known decay modes are modelled with EVTGEN [12] using the branching fractions taken from the Particle Data Group (PDG) [5], and the remaining unknown decays of the charmonium states are modeled by LUNDCHARM [13]. Final-state radiation is incorporated using the PHOTOS package [14].

The $D^0 \rightarrow K^+\pi^-\pi^0$ decay is simulated using an MC generator which combines the resonant decays $D^0 \rightarrow K^*(892)^0\pi^0$, $D^0 \rightarrow K^*(892)^+\pi^-$, $D^0 \rightarrow K^+\rho(770)^-$, and a three-body phase-space model. The $D^0 \rightarrow K^+\pi^-\pi^0\pi^0$ decay is simulated with a four-body phase-space model. The $D^0 \rightarrow K^-e^+\nu_e$ decay is simulated with the modified pole model [15] with the pole mass fixed at the D_s^{*+} nominal mass [5] and the other parameters quoted from [16].

III. MEASUREMENT METHOD

The center-of-mass energy of 3.773 GeV lies above the $D\bar{D}$ production threshold but below that of $D^*\bar{D}$. At this energy point, the $D^0\bar{D}^0$ pairs are produced copiously and are not accompanied by additional hadrons. This allows D decays to be studied with the double-tag method. In this analysis double-tag events refer to those in which the DCS decays $D^0 \rightarrow K^+\pi^-\pi^0$ or $D^0 \rightarrow K^+\pi^-\pi^0\pi^0$ are found on the recoiling side of the semileptonic decay $\bar{D}^0 \rightarrow K^+e^-\bar{\nu}_e$. The branching fraction of $D^0 \rightarrow K^+\pi^-\pi^0$ or $D^0 \rightarrow K^+\pi^-\pi^0\pi^0$ is determined by

$$\mathcal{B}_{\text{DCS}} = \frac{N_{\text{DT}}}{2 \cdot N_{D^0\bar{D}^0} \cdot \epsilon_{\text{DT}} \cdot \mathcal{B}_{\text{SL}}}, \quad (1)$$

where $N_{D^0\bar{D}^0} = (10597 \pm 28 \pm 98) \times 10^3$ is the total number of $D^0\bar{D}^0$ pairs in the data sample determined in our previous work [17], N_{DT} is the signal yield of the double-tag events obtained from the data sample, ϵ_{DT} is the effective efficiency of reconstructing the double-tag events, and \mathcal{B}_{SL} is the branching fraction of the semileptonic decay $\bar{D}^0 \rightarrow K^+e^-\bar{\nu}_e$ taken from the PDG [5].

IV. EVENT SELECTION

The double-tag candidates are required to contain at least two good photons for $D^0 \rightarrow K^+\pi^-\pi^0$ and four for $D^0 \rightarrow K^+\pi^-\pi^0\pi^0$ as well as exactly four charged tracks for both modes. We use the same selection criteria for K^\pm , π^\pm , e^- , and π^0 candidates as were used in our previous studies [3, 18–21]. All charged tracks are required to originate from a region within $|\cos\theta| < 0.93$, $|V_{xy}| < 1$ cm and $|V_z| < 10$ cm. Here, θ is the polar angle of the charged track with respect to the MDC axis,

$|V_{xy}|$ and $|V_z|$ are the distances of closest approach of the charged track to the interaction point perpendicular to and along the MDC axis, respectively. Particle identification (PID) of kaons and pions is performed with the combined dE/dx and TOF information to calculate their corresponding confidence levels. Charged tracks with confidence level for kaon (pion) hypothesis greater than that for pion (kaon) hypothesis are assigned as kaon (pion) candidates.

Photon candidates are selected by using the information recorded by the EMC. The shower time is required to be within 700 ns of the event start time. The shower energy is required to be greater than 25 (50) MeV if the crystal with the maximum deposited energy in that cluster is in the barrel (end-cap) region [8]. The opening angle between the shower direction and the extrapolated position on the EMC of the closest charged track must be greater than 10° . The π^0 candidates are formed by photon pairs with invariant mass within (0.115, 0.150) GeV/ c^2 . To improve the resolution, a kinematic fit constraining the $\gamma\gamma$ invariant mass to the π^0 known mass [5] is imposed on the selected photon pair.

In the selection of the $D^0 \rightarrow K^+\pi^-\pi^0\pi^0$ candidates, the invariant mass of the $\pi^0\pi^0$ combination is required to be outside of the interval (0.388, 0.588) GeV/ c^2 to reject the dominant peaking background from the singly Cabibbo-suppressed decay $D^0 \rightarrow K^+\pi^-K_S^0(\rightarrow \pi^0\pi^0)$. This requirement corresponds to about five standard deviations of the experimental K_S^0 mass resolution. The signal candidates for $D^0 \rightarrow K^+\pi^-\pi^0$ or $D^0 \rightarrow K^+\pi^-\pi^0\pi^0$ are identified with two variables: the energy difference

$$\Delta E \equiv E_{D^0} - E_{\text{beam}} \quad (2)$$

and the beam-constrained mass

$$M_{\text{BC}} \equiv \sqrt{E_{\text{beam}}^2 - |\vec{p}_{D^0}|^2}. \quad (3)$$

Here, E_{beam} is the beam energy, \vec{p}_{D^0} and E_{D^0} are the momentum and energy of the D^0 candidate in the e^+e^- rest frame, respectively. If there are multiple candidates for the hadronic side, only the one with the minimum $|\Delta E|$ is kept. The correctly reconstructed D^0 candidates concentrate around zero in the ΔE distribution and around the D^0 nominal mass in the M_{BC} distribution. The events satisfying $\Delta E \in (-54, 40)$ MeV for $D^0 \rightarrow K^+\pi^-\pi^0$ and $\Delta E \in (-60, 30)$ MeV for $D^0 \rightarrow K^+\pi^-\pi^0\pi^0$ are kept for further analysis.

After the hadronic D^0 mesons are reconstructed, the candidates for $\bar{D}^0 \rightarrow K^+e^-\bar{\nu}_e$ are selected from the remaining tracks that have not been used to select the hadronic side. Then, the number of extra charged tracks ($N_{\text{extra}}^{\text{charge}}$) is required to be zero. The charge of the electron candidate is required to be opposite to that of the kaon from the hadronic D^0 decay. Electron PID uses the combined dE/dx , TOF, and EMC information, with which the combined confidence levels under the

electron, pion, and kaon hypotheses (CL_e , CL_π , and CL_K) are calculated. Electron candidates are required to satisfy $CL_e > 0.001$ and $CL_e/(CL_e + CL_\pi + CL_K) > 0.8$. To reduce the background due to mis-identification between hadrons and electrons, the energy of the electron candidate deposited in the EMC is further required to be greater than 0.8 times its measured momentum. Then, to partially compensate the effects of final-state radiation and *bremsstrahlung* (FSR recovery), the four-momenta of photon(s) within 5° of the initial electron direction are added to the electron four-momentum measured by the MDC.

The charged kaons from the semileptonic decay are required to satisfy the same PID criteria as the kaons from the hadronic decays, and to have a charge opposite to that of the electron. To suppress potential backgrounds from hadronic decays with a misidentified electron, the invariant mass of the K^+e^- combination, $M_{K^+e^-}$, is required to be less than $1.8 \text{ GeV}/c^2$. Furthermore, we require that the maximum energy of extra photons ($E_{\text{extra}\gamma}^{\text{max}}$) which have not been used in the tag selection is less than 0.25 GeV and there is no extra π^0 candidate ($N_{\text{extra}\pi^0}$).

The semileptonic \bar{D}^0 decay is identified using a kinematic quantity defined as

$$U_{\text{miss}} \equiv E_{\text{miss}} - |\vec{p}_{\text{miss}}|. \quad (4)$$

Here, $E_{\text{miss}} \equiv E_{\text{beam}} - E_{K^+} - E_{e^-}$ and $\vec{p}_{\text{miss}} \equiv \vec{p}_{\bar{D}^0} - \vec{p}_{K^+} - \vec{p}_{e^-}$ are the missing energy and momentum of the double-tag event in the e^+e^- center-of-mass system, in which E_{K^+} and \vec{p}_{K^+} are the energy and momentum of the K^+ , and E_{e^-} and \vec{p}_{e^-} are the energy and momentum of the e^- candidate. The U_{miss} resolution is improved by constraining the D^0 energy to the beam energy and $\vec{p}_{\bar{D}^0} \equiv -\hat{p}_{D^0} \cdot \sqrt{E_{\text{beam}}^2 - M_{D^0}^2}$, where \hat{p}_{D^0} is the unit vector in the momentum direction of the D^0 and M_{D^0} is the D^0 nominal mass [5].

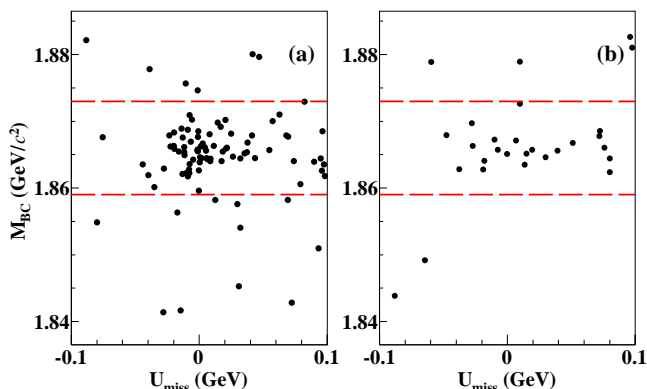


Fig. 1. Distributions of M_{BC} versus U_{miss} of the accepted double-tag candidate events for (a) $D^0 \rightarrow K^+\pi^-\pi^0$ and (b) $D^0 \rightarrow K^+\pi^-\pi^0\pi^0$ versus $\bar{D}^0 \rightarrow K^+e^-\bar{\nu}_e$ decays in data. The area between dashed red lines show the M_{BC} signal region.

Figure 1 shows the distributions of M_{BC} versus U_{miss} of the double-tag candidate events in data. The clusters around the known D^0 mass along the y axis and zero along the x axis are the signal double-tag candidate events. The signal region is selected around the known D^0 mass: those candidates satisfying $M_{\text{BC}} \in (1.859, 1.873) \text{ GeV}/c^2$ are kept for further analysis. After the implementation of the above-mentioned requirements, the U_{miss} distributions of the surviving events are shown in Fig. 2.

The detection efficiencies ϵ_{DT} obtained from signal MC samples are $(19.49 \pm 0.14)\%$ and $(5.56 \pm 0.07)\%$ for the double-tag events of $D^0 \rightarrow K^+\pi^-\pi^0$ and $D^0 \rightarrow K^+\pi^-\pi^0\pi^0$ versus $\bar{D}^0 \rightarrow K^+e^-\bar{\nu}_e$, respectively, where the efficiencies include the branching fraction of $\pi^0 \rightarrow \gamma\gamma$ and the uncertainties are statistical only.

The background components and corresponding ratios in the total background are described below. For $D^0 \rightarrow K^+\pi^-\pi^0$ versus $\bar{D}^0 \rightarrow K^+e^-\bar{\nu}_e$, the peaking backgrounds are mainly from the CF modes $D^0 \rightarrow K^-\pi^+\pi^0$ versus $\bar{D}^0 \rightarrow K^+e^-\bar{\nu}_e$ due to the mis-identification between kaons and pions in the hadronic side (36.0%) and the mis-identification between kaons and electrons in the hadronic side (12.9%); while the residual backgrounds are $D^0 \rightarrow K^-\pi^+\pi^0$ versus $\bar{D}^0 \rightarrow K^+e^-\bar{\nu}_e$ (7.9%), $D^0 \rightarrow K^+K^-$ versus $\bar{D}^0 \rightarrow K^+e^-\bar{\nu}_e$ (6.5%), $D^0 \rightarrow \bar{K}^0\pi^+\pi^-$ versus $\bar{D}^0 \rightarrow K^+e^-\bar{\nu}_e$ (5.8%) and other decay modes (30.9%). For $D^0 \rightarrow K^+\pi^-\pi^0\pi^0$ versus $\bar{D}^0 \rightarrow K^+e^-\bar{\nu}_e$, the peaking backgrounds are mainly from $D^0 \rightarrow K^-e^+\nu_e$ versus $\bar{D}^0 \rightarrow K^+\pi^-\pi^0\pi^0$ (30.6%); while the residual backgrounds are $D^0 \rightarrow K_S^0\pi^+\pi^-\pi^0$ versus $\bar{D}^0 \rightarrow K^+e^-\bar{\nu}_e$ (8.2%), $D^0 \rightarrow K^+K^-\pi^0$ versus $\bar{D}^0 \rightarrow K^+e^-\bar{\nu}_e$ (8.2%), $D^0 \rightarrow K_L^0\pi^+\pi^-$ versus $\bar{D}^0 \rightarrow K^+e^-\bar{\nu}_e$ (4.1%), and other decay modes (49.0%).

To measure the signal yields, unbinned maximum-likelihood fits are performed on the U_{miss} distributions. The non-peaking backgrounds (including a small contribution from wrongly reconstructed semileptonic candidates) are described by the corresponding MC-simulated shapes. The background shapes are derived from the inclusive MC sample and the signal shapes from the signal MC samples. The yield of the peaking background is fixed based on the known branching fractions and the mis-identification rates, and the yields of the signal and non-peaking backgrounds are free parameters of the fits. The fit results are shown in Fig. 2. From these fits, we measure $45.8_{-8.3}^{+9.0}$ signal events for the decay $D^0 \rightarrow K^+\pi^-\pi^0$ and $7.7_{-4.3}^{+5.0}$ signal events for $D^0 \rightarrow K^+\pi^-\pi^0\pi^0$. These results give the product branching fractions to be $\mathcal{B}(D^0 \rightarrow K^+\pi^-\pi^0) \cdot \mathcal{B}(\bar{D}^0 \rightarrow K^+e^-\bar{\nu}_e) = [1.11_{-0.20}^{+0.21}(\text{stat})] \times 10^{-5}$, and $\mathcal{B}(D^0 \rightarrow K^+\pi^-\pi^0\pi^0) \cdot \mathcal{B}(\bar{D}^0 \rightarrow K^+e^-\bar{\nu}_e) = [6.53_{-3.65}^{+4.24}(\text{stat})] \times 10^{-6}$. Combining the world average of $\mathcal{B}(\bar{D}^0 \rightarrow K^+e^-\bar{\nu}_e) = (3.541 \pm 0.034)\%$ [5], we obtain

$$\mathcal{B}(D^0 \rightarrow K^+\pi^-\pi^0) = [3.13_{-0.56}^{+0.60}(\text{stat})] \times 10^{-4},$$

and

$$\mathcal{B}(D^0 \rightarrow K^+\pi^-\pi^0\pi^0) = [1.84_{-1.00}^{+1.19}(\text{stat})] \times 10^{-4}.$$

The statistical significance of the signal is calculated by $\sqrt{-2\ln(\mathcal{L}_0/\mathcal{L}_{\max})}$, where \mathcal{L}_{\max} and \mathcal{L}_0 are the maximal likelihood of the fits with and without the signal contribution, respectively. These significances are determined to be 7.0σ and 1.9σ for $D^0 \rightarrow K^+\pi^-\pi^0$ and $D^0 \rightarrow K^+\pi^-\pi^0\pi^0$, respectively.

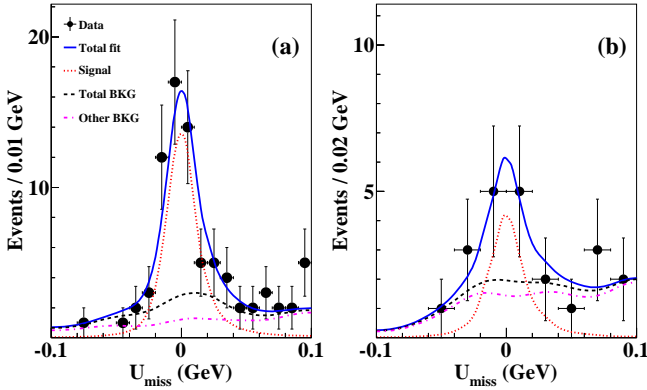


Fig. 2. Fits to the U_{miss} distributions of the accepted double-tag candidate events for (a) $D^0 \rightarrow K^+\pi^-\pi^0$ and (b) $D^0 \rightarrow K^+\pi^-\pi^0\pi^0$ versus $\bar{D}^0 \rightarrow K^+e^-\bar{\nu}_e$ decays. The points with error bars are data. The blue solid curves are the total fit results (Total fit). The red dotted and black dashed curves are the fitted signal (Signal) and background (Total BKG) components, respectively. The component between the black dashed and pink dot-dashed curves is the peaking background and the pink dot-dashed curve represents the other background contributions (Other BKG).

The upper limit on the branching fraction of the decay $D^0 \rightarrow K^+\pi^-\pi^0\pi^0$ is determined to be 3.6×10^{-4} at 90% confidence level, using the Bayesian approach [22] after incorporating the systematic uncertainty. The distribution of the likelihood versus the assumed branching fraction is shown in Fig. 3.

V. SYSTEMATIC UNCERTAINTIES

The systematic uncertainties originating from e^- tracking (PID) efficiencies are studied by using a control sample of $e^+e^- \rightarrow \gamma e^+e^-$ events. The efficiency ratios of data and MC simulation for e^- tracking and e^- PID are $(101.0 \pm 0.2)\%$ and $(101.2 \pm 0.2)\%$, respectively. Here, the two dimensional (momentum and $\cos\theta$) e^- tracking (PID) efficiencies from the control sample have been re-weighted to match those in the signal decays. The systematic uncertainties associated with the K^+ and π^- tracking (PID) efficiencies are investigated with $D^0 \rightarrow K^-\pi^+$, $K^-\pi^+\pi^0$, $K^-\pi^+\pi^+\pi^-$ versus $\bar{D}^0 \rightarrow K^+\pi^-$, $K^+\pi^-\pi^0$, $K^+\pi^-\pi^+\pi^-$, as well as $D^+ \rightarrow K^-\pi^+\pi^+$

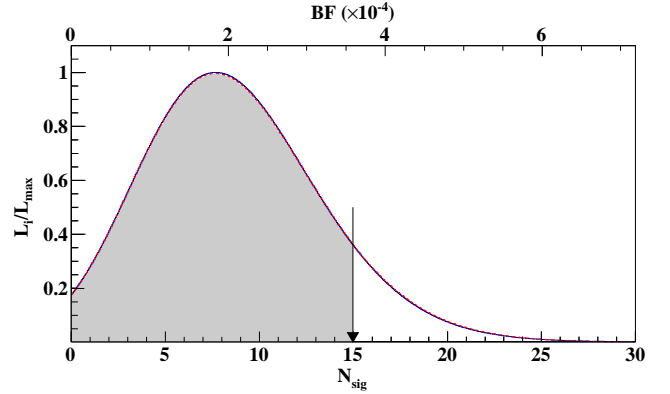


Fig. 3. Distributions of normalized likelihood distributions versus the signal yield N_{sig} and branching fraction of $D^0 \rightarrow K^+\pi^-\pi^0\pi^0$. The results obtained with and without incorporating the systematic uncertainty are shown by the red dashed and blue solid curves, respectively. The black arrow shows the result corresponding to 90% confidence level.

versus $D^- \rightarrow K^+\pi^-\pi^-$ double-tag hadronic $D\bar{D}$ events, using a sample with a missing K^+ or π^- . The ratios of tracking or PID efficiencies for charged kaons and pions between data and MC simulation are listed in Table 1. Here, the momentum dependent $K^+(\pi^-)$ tracking (PID) efficiencies from control samples have been re-weighted to match those in the signal decays. After correcting the signal MC efficiencies by these factors, the residual uncertainties on the tracking (PID) efficiencies of e^- , K^+ , and π^- are assigned as 0.2% (0.2%), 0.3% (0.2%), and 0.2% (0.2%), respectively.

Table 1. The ratios of efficiencies of K^+ tracking, K^+ PID, π^- tracking, and π^- PID between data and MC simulation.

Source	$D^0 \rightarrow K^+\pi^-\pi^0$ (%)	$D^0 \rightarrow K^+\pi^-\pi^0\pi^0$ (%)
K^+_{tracking}	101.1 ± 0.3	101.7 ± 0.3
K^+_{PID}	100.0 ± 0.2	100.0 ± 0.2
π^-_{tracking}	100.1 ± 0.2	100.2 ± 0.2
π^-_{PID}	99.6 ± 0.2	99.8 ± 0.2

The systematic uncertainty of π^0 reconstruction efficiency is investigated by using the double-tag hadronic $D\bar{D}$ decays of $\bar{D}^0 \rightarrow K^+\pi^-\pi^0$ and $\bar{D}^0 \rightarrow K^0_S\pi^0$ tagged by either $D^0 \rightarrow K^-\pi^+$ or $D^0 \rightarrow K^-\pi^+\pi^+\pi^-$ [18, 19]. The systematic uncertainty on the π^0 reconstruction efficiency is assigned as 0.8% for each π^0 .

The systematic uncertainty associated with the U_{miss} fit is estimated by comparing the baseline branching-fraction result with the result obtained with alternative signal shapes and background shapes. The systematic uncertainty due to the assumed signal shape is estimated by replacing the nominal description with one convolved with a Gaussian resolution function. Here, the parameters used in the convolved Gaussian function

representing the data-MC simulation difference are obtained from the CF decay $D^0 \rightarrow K^-\pi^+\pi^0(\pi^0)$. The change in the branching fraction due to the assumed signal shape is found to be negligible. The systematic uncertainty from the simulated background shape is taken into account by varying the dominant peaking background component by $\pm 1\sigma$. The change in the re-measured branching fraction, 1.0%, is assigned as the systematic uncertainty associated with the background shape for $D^0 \rightarrow K^+\pi^-\pi^0$ decays, while that for $D^0 \rightarrow K^+\pi^-\pi^0\pi^0$ decays, is found to be negligible. In addition, the effects of other background sources, examined by varying their size and shape, are also negligible.

The systematic uncertainties due to the requirements of ΔE and M_{BC} for the hadronic side as well as the requirement of $M_{K^+e^-}$ for the semileptonic side are studied by using control samples of the CF decay $D^0 \rightarrow K^-\pi^+\pi^0(\pi^0)$ versus $\bar{D}^0 \rightarrow K^+e^-\bar{\nu}_e$. The corresponding uncertainties are taken to be the differences of the acceptance efficiencies between data and MC simulation. These uncertainties are all found to be 0.1%. The systematic uncertainty associated with the K_S^0 veto in the $M_{\pi^0\pi^0}$ distribution is assigned by varying the mass window by ± 20 MeV/ c^2 . The maximum relative change in the measured branching fraction is not significantly larger than the statistical uncertainty after considering the correlations between the signal yields, hence this uncertainty is ignored [23].

The systematic uncertainty due to MC modeling is assigned to be the difference between the nominal efficiency and the average efficiency based on the signal MC events of the various components. Besides individual phase-space decays, the resonant decays $D^0 \rightarrow K^*(892)^0\pi^0$, $D^0 \rightarrow K^*(892)^+\pi^-$, and $D^0 \rightarrow K^+\rho(770)^-$ have been considered for $D^0 \rightarrow K^+\pi^-\pi^0$; and the resonant decays $D^0 \rightarrow K^*(892)^0\pi^0\pi^0$, $D^0 \rightarrow K^*(892)^+\pi^-\pi^0$, and $D^0 \rightarrow K^+\pi^0\rho^-$ have been considered for $D^0 \rightarrow K^+\pi^-\pi^0\pi^0$. The corresponding systematic uncertainties are assigned as 1.9% and 3.6% for $D^0 \rightarrow K^+\pi^-\pi^0$ and $D^0 \rightarrow K^+\pi^-\pi^0\pi^0$, respectively. The uncertainty in the MC modeling of the semileptonic decay of $\bar{D}^0 \rightarrow K^+e^-\bar{\nu}_e$ has been estimated in our previous work and is negligible [16].

The systematic uncertainty due to the $E_{\text{extra}\gamma}^{\text{max}}$, $N_{\text{extra}\pi^0}^{\text{charge}}$, and $N_{\text{extra}\pi^0}$ requirements is estimated by using a control sample of the CF decay $D^0 \rightarrow K^-\pi^+\pi^0(\pi^0)$ versus $\bar{D}^0 \rightarrow K^+e^-\bar{\nu}_e$. The differences in the acceptance efficiencies between data and MC simulation, 0.2% and 0.8%, are taken as the corresponding systematic uncertainties for the $D^0 \rightarrow K^+\pi^-\pi^0$ and $D^0 \rightarrow K^+\pi^-\pi^0\pi^0$ decays, respectively.

The uncertainties due to MC sample sizes are 0.7% and 1.2% for $D^0 \rightarrow K^+\pi^-\pi^0$ and $D^0 \rightarrow K^+\pi^-\pi^0\pi^0$ decays, respectively. The uncertainty from FSR recovery is estimated as 0.3% as in $\bar{D}^0 \rightarrow K^+e^-\bar{\nu}_e$ decays [16]. The total number of the $D^0\bar{D}^0$ pairs in the data sample is cited from Ref. [17] and is known with a precision that induces a systematic uncertainty of 0.9%. The branching

fraction of $\bar{D}^0 \rightarrow K^+e^-\bar{\nu}_e$ contributes a systematic uncertainty of 1.0% [5].

Adding all these uncertainties in quadrature yields a total systematic uncertainty of 2.9% for $D^0 \rightarrow K^+\pi^-\pi^0$ and 4.0% for $D^0 \rightarrow K^+\pi^-\pi^0\pi^0$. The systematic uncertainties discussed above are summarized in Table 2.

Table 2. Systematic uncertainties (in %) in the determination of the branching fractions.

Source	$K^+\pi^-\pi^0$	$K^+\pi^-\pi^0\pi^0$
Tracking of K^+ , e^- , and π^-	0.7	0.7
PID of K^+ , e^- , and π^-	0.5	0.5
π^0 reconstruction	0.8	1.6
K_S^0 veto	N/A	Ignored
MC model	1.9	3.6
U_{miss} fit	1.0	Negligible
ΔE requirement	0.1	0.1
M_{BC} requirement	0.1	0.1
$E_{\text{extra}\gamma}^{\text{max}} \& N_{\text{extra}\pi^0} \& N_{\text{extra}}^{\text{charge}}$	0.2	0.8
MC statistics	0.7	1.2
FSR recovery	0.3	0.3
$N_{D^0\bar{D}^0}$	0.9	0.9
Quoted branching fraction	1.0	1.0
Total	2.9	4.0

VI. SUMMARY

In conclusion, using 2.93 fb^{-1} of e^+e^- collision data accumulated at a center-of-mass energy of 3.773 GeV with the BESIII detector, we have measured the branching fraction of the DCS decay of $D^0 \rightarrow K^+\pi^-\pi^0$ and performed a search for the DCS decay $D^0 \rightarrow K^+\pi^-\pi^0\pi^0$. The branching fraction of $D^0 \rightarrow K^+\pi^-\pi^0$ is determined to be $[3.13_{-0.56}^{+0.60}(\text{stat}) \pm 0.09(\text{syst})] \times 10^{-4}$, which is consistent with the PDG value [5]. No significant signal is seen for $D^0 \rightarrow K^+\pi^-\pi^0\pi^0$ and an upper limit of 3.6×10^{-4} is set on the branching fraction at the 90% C.L. Using the world-average value of $\mathcal{B}(D^0 \rightarrow K^-\pi^+\pi^0) = (14.4 \pm 0.5)\%$ [5], we obtain the DCS/CF ratio $\mathcal{B}(D^0 \rightarrow K^+\pi^-\pi^0)/\mathcal{B}(D^0 \rightarrow K^-\pi^+\pi^0) = (0.22 \pm 0.04)\%$, corresponding to $(0.75 \pm 0.14)\tan^4\theta_C$. Our result for $D^0 \rightarrow K^+\pi^-\pi^0\pi^0$ and the world-average value of $\mathcal{B}(D^0 \rightarrow K^-\pi^+\pi^0\pi^0) = (8.86 \pm 0.23)\%$ [5] leads to the upper limit $\mathcal{B}(D^0 \rightarrow K^+\pi^-\pi^0\pi^0)/\mathcal{B}(D^0 \rightarrow K^-\pi^+\pi^0\pi^0) < 0.40\%$ at the 90% C.L., corresponding to $1.37 \times \tan^4\theta_C$. In the future, amplitude analyses of these two decays with larger data samples taken by BESIII [24, 25] can be used to measure the decay rates of the intermediate two-body D^0 decays, which are important for exploring quark SU(3)-flavor symmetry and its breaking effects, and thereby benefit the theoretical predictions of CP violation in hadronic D decays [26].

VII. ACKNOWLEDGEMENT

The BESIII collaboration thanks the staff of BEPCII and the IHEP computing center for their strong support. This work is supported in part by National Key Research and Development Program of China under Contracts Nos. 2020YFA0406400, 2020YFA0406300; National Natural Science Foundation of China (NSFC) under Contracts Nos. 12105076, 11705230, 11625523, 11635010, 11735014, 11822506, 11835012, 11935015, 11935016, 11935018, 11961141012, 12022510, 12025502, 12035009, 12035013, 12061131003, 12192260, 12192260, 12192261, 12192262, 12192263, 12192264, and 12192265; the Chinese Academy of Sciences (CAS) Large-Scale Scientific Facility Program; Joint Large-Scale Scientific Facility Funds of the NSFC and CAS under Contracts Nos. U1732263, U1832207; CAS Key Research Program of Frontier Sciences under Contract No. QYZDJ-

SSW-SLH040; 100 Talents Program of CAS; INPAC and Shanghai Key Laboratory for Particle Physics and Cosmology; ERC under Contract No. 758462; European Union's Horizon 2020 research and innovation programme under Marie Skłodowska-Curie grant agreement under Contract No. 894790;; German Research Foundation DFG under Contracts Nos. 443159800, Collaborative Research Center CRC 1044, FOR 2359, GRK 214; Istituto Nazionale di Fisica Nucleare, Italy; Ministry of Development of Turkey under Contract No. DPT2006K-120470; National Science and Technology fund; Olle Engkvist Foundation under Contract No. 200-0605; STFC (United Kingdom); The Knut and Alice Wallenberg Foundation (Sweden) under Contract No. 2016.0157; The Royal Society, UK under Contracts Nos. DH140054, DH160214; The Swedish Research Council; U. S. Department of Energy under Contracts Nos. DE-FG02-05ER41374, DE-SC-0012069.

-
- [1] H. Y. Cheng and C. W. Chiang, *Phys. Rev. D* **81**, 074021 (2010).
 - [2] H. J. Lipkin, *Nucl. Phys. Suppl.* **115**, 117 (2003).
 - [3] M. Ablikim *et al.* (BESIII Collaboration), *Phys. Rev. Lett.* **125**, 141802 (2020).
 - [4] M. Ablikim *et al.* (BESIII Collaboration), [arXiv:2105.14310](https://arxiv.org/abs/2105.14310) [hep-ex].
 - [5] P. A. Zyla *et al.* (Particle Data Group), *Prog. Theor. Exp. Phys.* **2020**, 083C01 (2020).
 - [6] M. Ablikim *et al.* (BESIII Collaboration), *Chin. Phys. C* **37**, 123001 (2013); *Phys. Lett. B* **753**, 629 (2016).
 - [7] Z. Z. Xing, *Phys. Rev. D* **55**, 196 (1997).
 - [8] M. Ablikim *et al.* (BESIII Collaboration), *Nucl. Instrum. Meth. A* **614**, 345 (2010).
 - [9] C. H. Yu *et al.*, *Proceedings of IPAC2016, Busan, Korea, 2016*.
 - [10] S. Agostinelli *et al.* (GEANT4 Collaboration), *Nucl. Instrum. Meth. A* **506**, 250 (2003).
 - [11] S. Jadach, B. F. L. Ward, and Z. Was, *Comp. Phys. Comm.* **130**, 260 (2000); *Phys. Rev. D* **63**, 113009 (2001).
 - [12] D. J. Lange, *Nucl. Instrum. Meth. A* **462**, 152 (2001); R. G. Ping, *Chin. Phys. C* **32**, 599 (2008).
 - [13] J. C. Chen, G. S. Huang, X. R. Qi, D. H. Zhang, and Y. S. Zhu, *Phys. Rev. D* **62**, 034003 (2000).
 - [14] E. Richter-Was, *Phys. Lett. B* **303**, 163 (1993).
 - [15] D. Becirevic and A. B. Kaidalov, *Phys. Lett. B* **478**, 417 (2000).
 - [16] M. Ablikim *et al.* (BESIII Collaboration), *Phys. Rev. D* **92**, 072012 (2015).
 - [17] M. Ablikim *et al.* (BESIII Collaboration), *Chin. Phys. C* **42**, 083001 (2018).
 - [18] M. Ablikim *et al.* (BESIII Collaboration), *Eur. Phys. J. C* **76**, 369 (2016).
 - [19] M. Ablikim *et al.* (BESIII Collaboration), *Chin. Phys. C* **40**, 113001 (2016).
 - [20] M. Ablikim *et al.* (BESIII Collaboration), *Phys. Rev. Lett.* **123**, 231801 (2019).
 - [21] M. Ablikim *et al.* (BESIII Collaboration), *Phys. Rev. D* **102**, 112005 (2020).
 - [22] K. Stenson, [arXiv:physics/0605236](https://arxiv.org/abs/physics/0605236) [physics.data-an].
 - [23] R. Barlow, [arXiv:hep-ex/0207026](https://arxiv.org/abs/hep-ex/0207026).
 - [24] M. Ablikim *et al.* (BESIII Collaboration), *Chin. Phys. C* **44**, 040001 (2020).
 - [25] H. B. Li and X. R. Lyu, *Natl. Sci. Rev.* **8**, nwab181 (2021).
 - [26] M. Saur and F. S. Yu, *Sci. Bull.* **65**, 1428 (2020).